SEA-SURFACE SCATTERING OF A CONTINUOUS WAVE IN THE 1 TO 200 HZ FREQUENCY RANGE

Iannis Bennaceur[a], Xavier Cristol[a]

[a]THALES Defense Mission Systems FRANCE

525 route des Dolines, 06560 Valbonne FRANCE.
iannis.bennaceur@fr.thalesgroup.com

Abstract: *The purpose of this paper is the scattering of a continuous wave in the 1 to 200 Hz low frequency range by the fully developed swell of the Atlantic Ocean in a deep-water configuration. Considering the scales of the problem, we use the small-perturbation method coupled with the normal-mode theory and an asymptotic analysis to derive the first order spatio-temporal scattered pressure field p_1. This approach, greatly inspired by Labianca and Harper, allows us to express p_1 depending on the normal-mode functions and their associated wave-numbers that we compute numerically using an in-house modal propagation code called MOCTESUMA. This code may be run for an ocean waveguide with any particular sound-speed profile and takes into account the propagation into multiple-layers sea-bottom. First, we compare the computed power spectral density of pressure fluctuations with the one measured experimentally in the Sargasso Sea [1]. In a second phase we compare the propagation losses undergone by the scattered field and the non-perturbed field in the shadow zone appearing when the acoustic source is located in the summer thermocline. Finally we look at the level of scattered energy on both sides of the scattering mechanism cut-off ratio $\Gamma/k_0 = 2$, depending on the source immersion.*

Keywords: *Underwater acoustic modelling, sea-surface scattering, low-frequency range, deep-water acoustic propagation*

1. INTRODUCTION AND METHOD

The scattering of acoustic waves by rough surfaces has been widely studied in the past decades [2] and results to amplitude and phase modulation as well as a spatial and spectral re-distribution of the acoustic energy. The resolution method for a scattering problem depends both on the emitted wave and on the rough surface scales. In this study, we consider the scattering of low-frequency emissions (f_0 from 1 to 200 Hz meaning a wavelength λ_0 varying between 7.5 and 1500 m) by the fully developed swell which typical scales h and L, respectively the root-mean square value of the surface height fluctuations and their horizontal scale, vary from 1.3 10^{-3} to 1.2 m and from 0.21 to 200 m depending on the sea-state. Since $h/\lambda_0 \ll 1$ and $h/L \ll 1$, we use the small perturbation method. This method consists in evaluating the first terms of the perturbed pressure field Taylor development with h as small parameter. Here we focus on the computation of the first order term p_1 which gives a good approximation of the energy re-distributed on frequencies adjacent to the carrier.

We have followed [3] to derive the exact integral solution of the scattered pressure field p_1 (cf. equation 15(b) of [3]) before leading the same asymptotic analysis as [4] valid for source-receiver distances higher than 2.5 km, using equation (2) p.399 of [5] to obtain a simplified expression for p_1. The derivation of p_1 is made under the hypothesis that the swell is a sinusoidal wave $u(x,t) = 2\cos(\Gamma x - \Omega t)$ with Γ and Ω respectively the wave-number and pulsation of the swell that propagates in the $\boldsymbol{e}_x$ direction at the velocity $V_S = g/\Omega$ with g the gravity constant. Furthermore, the source and acoustic receiver are static. The major difference with previous works ([3], [4], [6] and [7]) lies in the use of the in-house modal propagation code MOCTESUMA for the computation of modal functions $u_m(\omega)$ and associated wavenumbers $K_m(\omega)$ of ocean waveguides with any particular sound-speed profile. Also we add an imaginary part in $K_m(\omega)$ enabling the convergence of the computation and we do not consider that $\omega_0 \pm \Omega \approx \omega_0$ anymore.

2. RESULTS

The total pressure field, truncated at the first order term in h, may be expressed as :

$$p(\boldsymbol{r},t) = p_0(\boldsymbol{r},t) + hp_1(\boldsymbol{r},t) = T_0(\boldsymbol{r})\mathrm{e}^{-i\omega_0 t} + T_1^-(\boldsymbol{r})\mathrm{e}^{-i(\omega_0-\Omega)t} + T_1^+(\boldsymbol{r})\mathrm{e}^{-i(\omega_0+\Omega)t} \quad (1)$$

where the quantities T_0, T_1^- and T_1^+ respectively give the level of energy at the source frequency ω_0 and within the side-lobes centred at $\omega_0 \pm \Omega$. All the computations have been realised with a seabed that presents a relatively soft muddy first layer with a porosity of 65%, a density of 1.41 tonne/m^3 and an upper velocity of compression P-waves of 1534 m/s.

2.1. Comparison to Shooter & Mitchell measurements

The authors in ref. [1] have conducted an experiment in the Sargasso Sea during the summer period to highlight the effect of the scattering of a continuous wave (CW) by the agitated sea-surface. They have hauled an acoustic source immersed at 18 m, emitting at 138 Hz, at a speed of 5 knots and computed the power spectral densities (PSD) of pressure fluctuations received at a depth of 3411 (cf. *Fig 1(a)*) and 4789 m. They have showed the spectral re-distribution of the acoustic energy into side-lobes, located between 0.1 and 0.2 Hz away from the Doppler shifted source frequency, which are typical frequencies of the swell.

Moreover, the PSD exhibits a dissymmetry between the levels of its two side-lobes due to the fact that the receiver is more deeply immersed than the source.

For the purpose of supporting our theoretical and numerical approach, we have computed the PSD of the pressure field expressed by (1) in a configuration as close as the one of the experimental campaign in order to compare the level of the side-lobes. According to the environmental data described in [1], we have estimated the sea-state to be around 4 and 5 during the experiment, meaning a wind speed of 10.3 m. Using the JONSWAP model, we have computed the pressure field with $\Omega = 0.84$ rad/s, $h = 0.54$ m and $\Gamma = 0.072$ m^{-1}. *Fig. 1(b)* shows the computed spatially averaged spectra, artificially shifted by -0.23 Hz to take into account the Doppler effect, along with a measure of the spatial spectra's dispersion. The level of the right side-lobe is very close to the experimental one whereas the level of the left side-lobe is a bit lower. Furthermore, our computation exhibits the same side-lobes level dissymmetry.

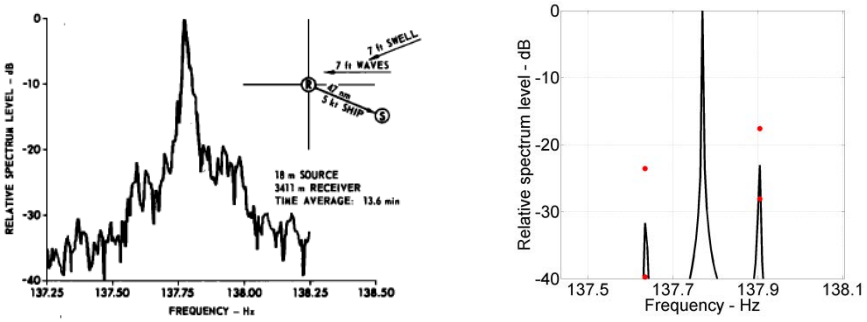

(a) *(b)*

Fig.1: Power spectral densities (a) from [7] and (b) computed.

2.2. Shadow zone filling by the scattered pressure field

In this section we compute the terms T_0, T_1^- and T_1^+ of eq. (1) with a deep-water, north Atlantic sound-speed profile during the summer period, with a source immersed at $z_0 = 5$ m emitting at $f_0 = 50$ or 180 Hz and a receiver immersed at $z_R = 300$ m. We choose a sea-state of 3 leading to $\Omega = 1.6$ rad/s, $h = 0.15$ m and $\Gamma = 0.26$ m^{-1}. *Fig.2(a)* represents the propagation losses in the vertical plane if the sea were perfectly flat ($-20\log_{10}|4\pi T_0|$) for a source emitting at 180 Hz. We observe a strong shadow zone spreading from 3 km to 20 km in range and from 0 to 1000 m in depth and a strong decrease of the propagation losses around 60 km, region called the first convergence zone. *Fig.2(b)* represents the propagation losses in the horizontal plane, the source being located at $x_0 = y_0 = 0$ m. Since the sound-speed profile is uniform in this plane, the propagation losses present a revolution symmetry around the source location. We clearly observe the shadow zone for the radii between 3 and 20 km as well as the first convergence zone around 60 km.

Let us focus now on the scattered pressure field. We plot on *Fig.3* the propagation losses related to the left side-lobe ($-20\log_{10}|4\pi T_1^-|$) in the horizontal plane for the source emitting at 50 and 180 Hz. We recall that the swell progresses in the $\boldsymbol{e}_x$ direction. At 50 Hz, we see that the level of scattered energy is relatively high (low propagation losses) for a specific angle of aperture with respect to the swell propagation direction and strongly decreases after a "*critical angle*" $\theta_c \approx \pm 54°$. The spatial distribution of the scattered energy for the $x > 0$ looks like the one for the $x < 0$ but is not exactly the same since the plane $x = 0$ is not a plane of symmetry. At 180 Hz, θ_c is higher, approximately equal to ±81° and the scattered energy level difference on both sides of the *critical angle* is lower. Furthermore, we notice that the level of scattered energy is globally higher in the directions defined by the *critical angle* than elsewhere, especially for distances lower than 15 km. Finally, we observe that the level of scattered energy increases around the first convergence zone.

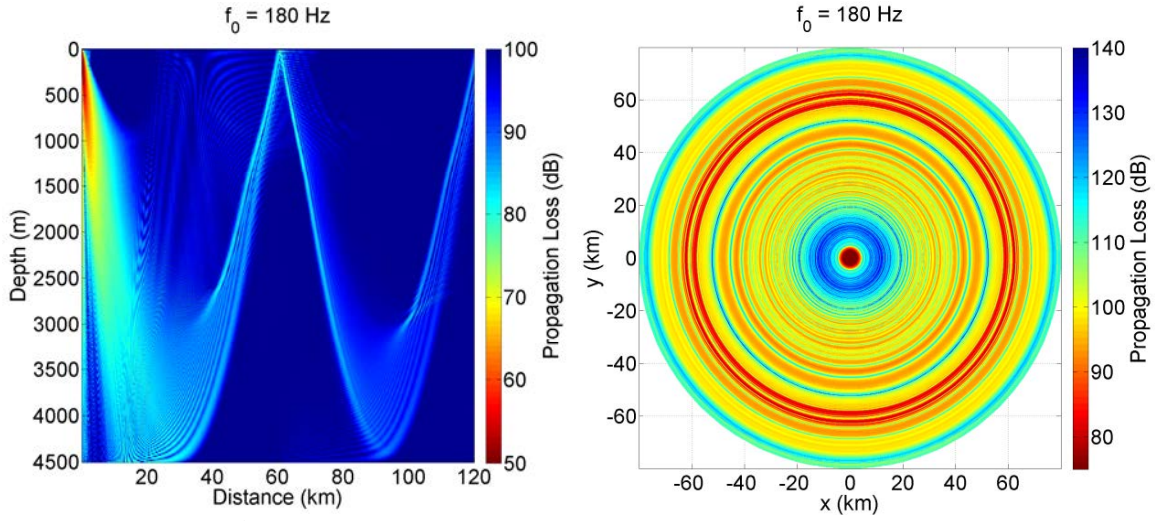

(a) *(b)*

Fig.2: Propagation losses for a source emitting at 180 Hz in (a) the vertical and (b) the horizontal plane.

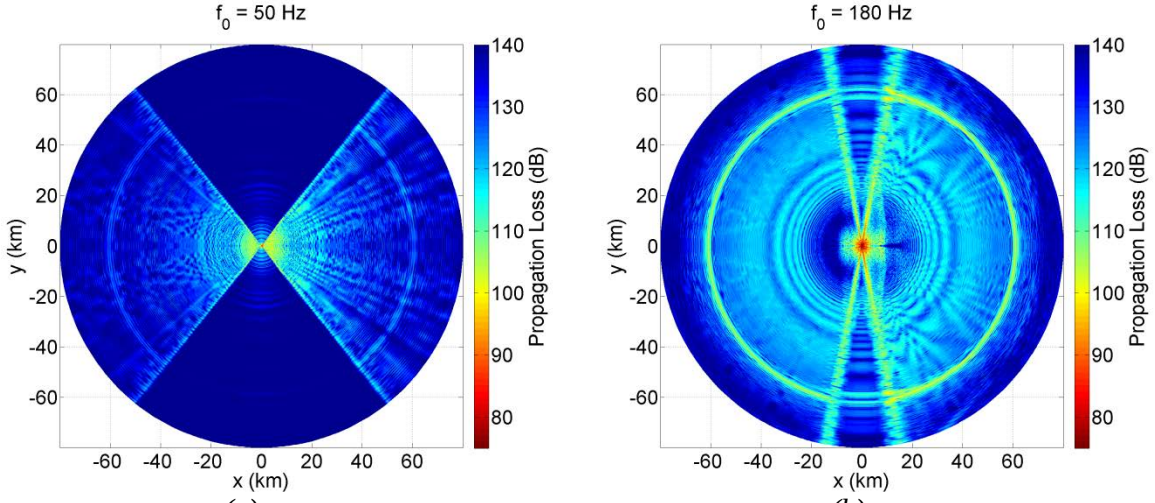

(a) *(b)*

Fig.3: Propagation losses of the left side-lobe for (a) f_0 =50 and (b) f_0 =180 Hz.

We have noticed that the *critical angle* is close to the Bragg resonance angle $\psi = \operatorname{acos} \Gamma/2k_0$, whose definition and physical implications are illustrated in [9]. Considering that the grazing angle of incident rays on the sea-surface are low ($k_{iz}^* \to 0$) according to the considered source-receiver distances, we find, using the wave-number diagrams approach [8], that a necessary condition for the first order scattering to occur is that $k_{ix}^* > \Gamma/2k_0$ inducing $\theta < \psi$ with k_{ix}^* the normalized incident wave-number component in the $\boldsymbol{e}_x$ direction.

We now compare the propagation losses undergone by the pressure field p_0 with the ones undergone by the scattered pressure field at $f_0 - \Omega$ inside the shadow zone by plotting on *Fig.4* the quantity $\Delta^- = -20 \log_{10} |T_1^-/T_0|$ in a dB scale. We have assigned the value $\Delta^- = 0$ when the propagation losses associated with the left side-lobe are higher than 100 dB in order to focus only on the relatively low level of propagation losses. We then observe that the level of propagation losses associated with hp_1 is, in the directions of the critical angle, 5 to 30 dB lower than the ones of p_0 for a source-receiver distance going from 5 to 20 km. This means that the shadow zone is filled up by the scattered pressure field on the critical angle directions. This may have an impact on detection in the shadow zone; an array processing may fail to detect at f_0 whereas it would have detected at $f_0 - \Omega$. Such filling is observed, on a smaller scale, from $f_0 = 130$ Hz. The truthfulness of such observation may be questionable since, in the small-perturbation theory, hp_1 is supposed to always be way lower than p_0. This is indeed

the case for the vast majority of receiver positions, frequencies and environmental configurations tested but our approach may still fail when getting close to the *critical angle*. It would be worth validating this observation, either with another theoretical approach or with a dedicated experiment.

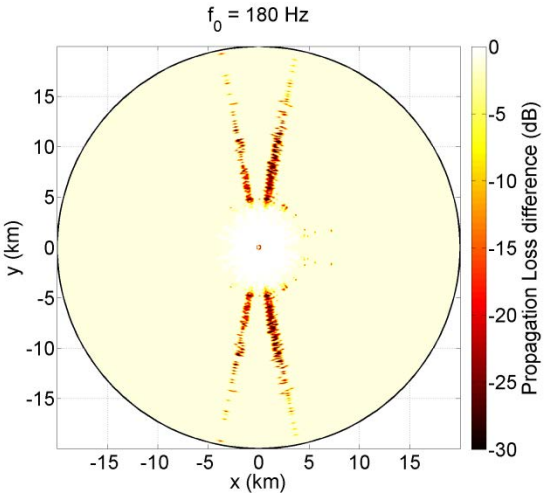

Fig.4: $-20\log_{10}|T_1^-/T_0|$ *for* f_0 *=180 Hz.*

2.3. Cut-off frequency of the scattering mechanism

Fig.5 represents 4π times T_0, T_1^- and T_1^+ computed for a source immersed at 5 and 300 m against f_0 at the receiving position (x_R, y_R, z_R) = (60,0,0.3) km, in the same environmental configuration than the previous section. At this receiving location, the scattered energy remains 20 to 40 dB lower than the energy carried at f_0, depending on the source frequency and immersion. Furthermore, for $z_0 = 300$ m, we notice a strong increase of about 40 dB of the scattered energy at $f_0 = 30$ Hz. At this frequency, the ratio $\Gamma/k_0 \approx 2$. The authors in [8] had already identified this cut-off value from which the first order term p_1 is drastically reduced and gave a physical interpretation based on wave-number diagrams and ray trajectories. When we consider a source immersed at 5 m (*Fig.5(a)*), we observe that the level of scattered energy decrease in a more progressive way, especially the right side-lobe.

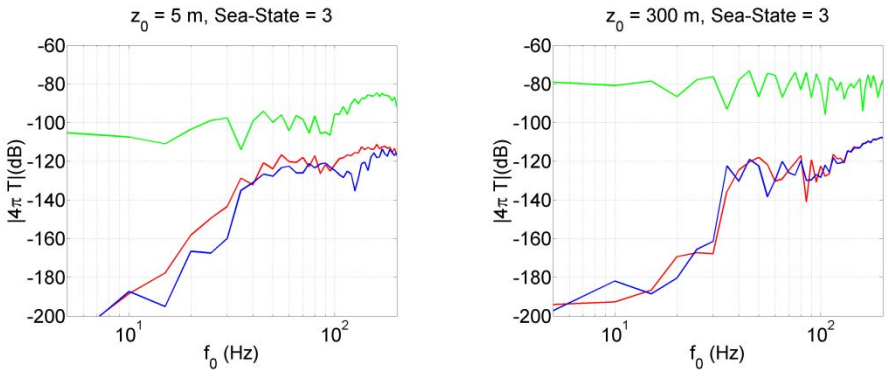

(a) *(b)*

Fig.5: T_0*: (---),* T_1^-*: (---) and* T_1^+*: (---) against* f_0 *for a source immersed at (a) 5 and (b) 300 m.*

To have a better look at the scattered energy decrease on both sides of the cut-off ratio, we plot on *Fig.6* $|4\pi T_1^+|$ against Γ/k_0 for the sea-states 1, 3 and 5. For the source immersed at 300 m, the decline of the scattered energy is significant when Γ/k_0 is exceeded, especially when the sea-state is equal to 1 or 3, whereas it is smoother when the source is located in the thermocline. At this time, we are not able to explain this observation.

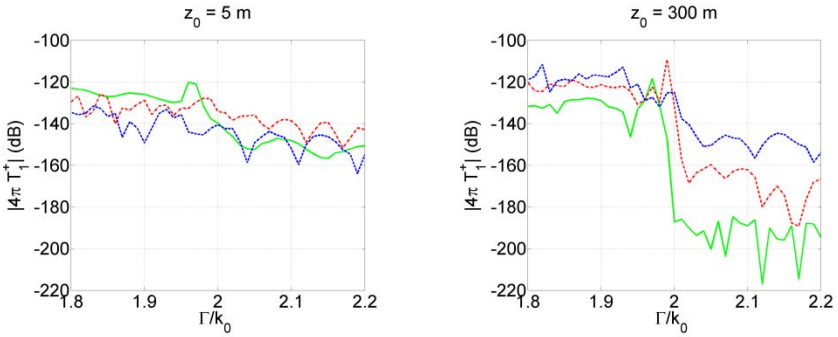

(a) *(b)*

Fig.3: T_1^+ computed for sea-states equal to 1:(---), 3:(-- --) and 5: (- · -) against Γ/k_0 for a source immersed at (a) 5 and (b) 300 m.

5. CONCLUSION

In this paper we studied the scattering of a continuous wave in the 1 to 200 low frequency range by the fully developed swell of the Atlantic Ocean in deep-water configurations. We used the small-perturbation method coupled with the normal-mode theory and an asymptotic analysis to derive the first order spatio-temporal scattered pressure field p_1. Our approach splits off from [3] by the use of an in-house code that provides the modal functions allowing the computation of p_1 for any waveguides. As a first step, we compared favorably the side-lobes level issued from our computation with the ones measured experimentally by [1] in the Sargasso Sea. Then we showed that the shadow zone observed when the source is located in the summer thermocline is filled up by the scattered pressure field from 130 Hz, on the directions defined by the Bragg resonance angle. Finally, we showed that the collapse of p_1 when $\Gamma/k_0 > 2$ may be relatively smooth when the source is located in the thermocline.

6. REFERENCES

[1] **Shooter J. A., Mitchell S. K.**, Observations of acoustics sidebands in cw tones received at long ranges, *J. Acoust. Soc. Am.*, volume (90), pp. 829-832, 1975.

[2] **Voronovitch A. G.**, *Wave scattering from Rough Surfaces*, Berlin: Springer-Verlag, 1994.

[3] **Labianca F. M., Harper E. Y.**, Connection between various small-waveheight solutions of the problem of scattering from the ocean surface, *J. Acoust. Soc. Am.*, volume (62), pp. 1144-1157, 1977.

[4] **Labianca F. M., Harper E. Y.**, Sideband structure of sound from a harmonic point source scattered by a rough surface moving over an upward-refracting ocean, *J. Acoust. Soc. Am.*, volume (61), pp. 378-389, 1977.

[5] **Felsen L. B., Marcuvitz N.**, *Radiation and Scattering of Waves.* New York: Wiley-IEEE Press, 1994.

[6] **Harper E. Y., Labianca F. M.**, Perturbation theory for scattering of sound from a point source by a moving rough surface in the presence of refraction, *J. Acoust. Soc. Am.*, volume (57), pp. 1044-1051, 1975.

[7] **Harper E. Y., Labianca F. M.**, Scattering of sound from a point source by a rough surface progressing over an isovelocity ocean, *J. Acoust. Soc. Am.*, volume (58), pp. 349-364, 1975.

[8] **Labianca F. M., Harper E. Y.**, Asymptotic theory of scattering by a rough surface progressing over an inhomogeneous ocean, *J. Acoust. Soc. Am.*, volume (59), pp. 799-812, 1976.